

Contents lists available at ScienceDirect

NanoImpact

journal homepage: www.elsevier.com/locate/nanoimpact





Improving the dichloro-dihydro-fluorescein (DCFH) assay for the assessment of intracellular reactive oxygen species formation by nanomaterials

Nienke Ruijter^a, Margriet van der Zee^{a,b}, Alberto Katsumiti^c, Matthew Boyles^{d,e}, Flemming R. Cassee^{a,f,*}, Hedwig Braakhuis^{a,g}

- ^a National Institute for Public Health & the Environment (RIVM), 3721 MA Bilthoven, the Netherlands
- ^b Science Lines, Emmalaan 8, 3451 CT Vleuten, the Netherlands
- ^c GAIKER Technology Centre, Basque Research and Technology Alliance (BRTA), 48170 Zamudio, Spain
- ^d Institute of Occupational Medicine (IOM), Edinburgh, EH14 4AP, UK
- e Centre for Biomedicine and Global Health, School of Applied Sciences, Edinburgh Napier University, Sighthill Campus, Edinburgh EH11 4BN, UK
- f Institute for Risk Assessment Sciences (IRAS), Utrecht University, 3584 CS Utrecht, the Netherlands
- ⁸ TNO Risk Analysis for Products in Development, 3584 CB Utrecht, the Netherlands

ARTICLE INFO

Editor: Phil Demokritou

Keywords:
Dichloro-dihydro-fluorescein assay
DCFH assay
Reactive oxygen species
ROS
Oxidative stress
SSbD
Hazard screening

ABSTRACT

To facilitate Safe and Sustainable by Design (SSbD) strategies during the development of nanomaterials (NMs), quick and easy *in vitro* assays to test for hazard potential at an early stage of NM development are essential. The formation of reactive oxygen species (ROS) and the induction of oxidative stress are considered important mechanisms that can lead to NM toxicity. *In vitro* assays measuring oxidative stress are therefore commonly included in NM hazard assessment strategies. The fluorescence-based dichloro-dihydro-fluorescein (DCFH) assay for cellular oxidative stress is a simple and cost-effective assay, making it a good candidate assay for SSbD hazard testing strategies. It is however subject to several pitfalls and caveats. Here, we provide further optimizations to the assay using 5-(6)-Chloromethyl-2',7'-dichlorodihydrofluorescein diacetate acetyl ester (CM-H₂DCFDA-AE, referred to as DCFH probe), known for its improved cell retention.

We measured the release of metabolic products of the DCFH probe from cells to supernatant, direct reactions of $CM-H_2DCFDA-AE$ with positive controls, and compared the commonly used plate reader-based DCFH assay protocol with fluorescence microscopy and flow cytometry-based protocols. After loading cells with DCFH probe, translocation of several metabolic products of the DCFH probe to the supernatant was observed in multiple cell types. Translocated DCFH products are then able to react with test substances including positive controls. Our results also indicate that intracellularly oxidized fluorescent DCF is able to translocate from cells to the supernatant. In either way, this will lead to a fluorescent supernatant, making it difficult to discriminate between intra-and extra-cellular ROS production, risking misinterpretation of possible oxidative stress when measuring fluorescence on a plate reader.

The use of flow cytometry instead of plate reader-based measurements resolved these issues, and also improved assay sensitivity. Several optimizations of the flow cytometry-based DCFH ISO standard (ISO/TS 19006:2016) were suggested, including loading cells with DCFH probe before incubation with the test materials, and applying an appropriate gating strategy including live-death staining, which was not included in the ISO standard.

In conclusion, flow cytometry- and fluorescence microscopy-based read-outs are preferred over the classical plate reader-based read-out to assess the level of intracellular oxidative stress using the cellular DCFH assay.

^{*} Corresponding author at: Antonie van Leeuwenhoeklaan 9, 3721 MA Bilthoven, the Netherlands. *E-mail address*: Flemming.cassee@rivm.nl (F.R. Cassee).

1. Introduction

The number and quantities of new nanomaterials (NMs) that enter the market and the number of NM applications are steadily increasing (Inshakova and Inshakov, 2017). From one substance or material, a virtually infinite number of nanoforms (NFs) can be synthesised, for instance, by tuning the size or shape or by applying coatings. The vast variety and quick development of new NFs has created a challenge for regulators and risk assessors to keep up with assessing their potential toxicity. A safe and sustainable by design (SSbD) approach supports the design and development of SSbD materials and involves performing risk assessment during the early stages of NM development to ensure safety along the entire life cycle (development, use, and end-of-life) (Caldeira et al., 2022; OECD, 2020; Soeteman-Hernandez et al., 2019). Early hazard screening in the context of SSbD may help to streamline risk assessment of NMs and accelerate innovation of nano-enabled products (NEPs). Within the EU-project SAbyNA, academic, industrial and governmental stakeholders collaborate to develop a SSbD approach for NMs and NEPs. Since SSbD involves hazard assessment during the early phases of product development, reliable, sensitive and easy-to-use in vitro, often cell based, tests present a useful tool for this approach (Ruijter et al., 2023; Zielinska et al., 2020). Such methods are not only valuable for SSbD, but also for grouping and read-across purposes, as well as for other hazard screening requirements (Stone et al., 2020).

Oxidative potential (OP), reactive oxygen species (ROS) formation, and induction of oxidative stress (OS), are considered to be important drivers of NM toxicity, and are therefore often included in NM specific hazard assessment strategies (Dekkers et al., 2016; Dekkers et al., 2020), grouping approaches (Arts et al., 2015; Braakhuis et al., 2021; Di Cristo et al., 2021), and suggested adverse outcome pathway networks (Braakhuis et al., 2020; Halappanavar et al., 2021). Due to their small size and relatively large surface area, NMs have a relatively high potential to induce ROS and reactive nitrogen species (RNS) formation in their direct surroundings. Examples of ROS are the short-lived hydroxide radicals (OH-) and superoxide anion (O2•), and the longer-lived hydrogen peroxide (H2O2). Despite being a natural product of mitochondrial oxidative metabolism and playing a role in essential cellular signalling systems, a chronic excess of ROS can be damaging, and is associated with several diseases such as fibrosis and cancer (Richter and Kietzmann, 2016; Saikolappan et al., 2019). Mammalian cells possess extensive antioxidant defence mechanisms against ROS, but if the oxidative burden becomes too large, the cell will turn to a state of oxidative stress. The excess of ROS oxidize the surrounding biomolecules and lipids in a chain reaction, causing cell damage, inflammation, and possibly DNA damage (Fu et al., 2014). This phenomenon has been observed for many types of NMs like TiO2 (Braakhuis et al., 2020), transition metals (Abdal Dayem et al., 2017), SiO₂ (Croissant et al., 2020; van Berlo et al., 2010), and carbon based NMs (Koike and Kobayashi, 2006; Reddy et al., 2011).

A number of acellular reactivity assays exist that can directly measure the oxidative potential of NMs (Ag Seleci et al., 2022; Boyles et al., 2022). However, measuring oxidative stress or ROS production in a cellular environment captures a wider range of toxic effects, as well as the cells' abilities to cope with them (Ayres et al., 2008; Hellack et al., 2017). Generally speaking, cellular ROS and OS assays are better capable of predicting *in vivo* effects than acellular OP assays (Bahl et al., 2020; Hellack et al., 2017; Riebeling et al., 2016). However, cellular assays measuring oxidative damage such as lipid peroxidation or protein carbonylation are likely too complex for low-tier early hazard assessment or hazard screening (Ruijter et al., 2023). The cellular DCFH assay is a simpler and widely used alternative.

In this paper, the optimization of the cellular dichloro-dihydro-fluorescein (DCFH) assay is described. The DCFH assay measures intracellular ROS production by forming a fluorescent product (DCF) upon oxidation by free radicals. In the DCFH assay, the parent compound added to the cell culture (available as *i.a.* DCFH-DA, H₂DCFDA, or

CM-H₂DCFDA), commonly called the DCFH probe, is considered unresponsive to free radicals until its conversion by intracellular esterases, which is also supposed to ensure its intracellular retention. The classical procedure of this assay is simple, quick, and is often performed using a spectrophotometer to detect the fluorescence of DCF. Macrophages are a common choice of cell type for this assay, due to their important role in the clearance of NMs, and their high abundance throughout the body. Although, the assay has been shown to be effective in many other cell types. The DCFH probe is quite unspecific when it comes to ROS detection and can be oxidized by a wide variety of ROS and RNS, making the assay suitable for determining a general level of ROS and RNS (Kalyanaraman et al., 2012). However, the usefulness of the data derived when using the DCFH assay has already been questioned for some time (Kalyanaraman et al., 2012; Murphy et al., 2022).

Recently, much effort has been put into optimizing in vitro toxicity assays for their use with NMs. For most if not all NMs their autofluorescence, high adsorption capacity, catalytic activity, and optical properties may be beneficial for their intended application, but also complicate the use of a number of toxicity assays, and creates a need for adjustments of protocols and inclusion of additional controls (Gulumian and Cassee, 2021; Joris et al., 2013; Kroll et al., 2012; Ribeiro et al., 2017). The DCFH assay is a promising tool when it comes to measuring intracellular ROS, although pitfalls for this assay have already been noted when applying it to assess the potency of NMs to induce ROS. Firstly, since the read-out of the assay is a fluorescent signal, particles with auto-fluorescing or quenching properties may cause interference (Aranda et al., 2013). Secondly, one-electron oxidation of DCFH leads to an intermediate form, DCF \bullet -, which is able to react with O_2 to form O_2^{\bullet} , artificially amplifying the fluorescent signal (Folkes et al., 2009; Wardman, 2007; Zhang and Gao, 2015). Thirdly, DCFH is susceptible to photo-oxidation, resulting in an overestimation of the signal when exposed to light. And finally, oxidized DCF is susceptible to photobleaching, reducing the fluorescent signal upon light exposure (Zhang and Gao, 2015). Taken together, there are various reasons why the outcomes of this assay should be interpreted with caution. A good step towards optimization and harmonization was made when ISO published ISO/TS 19006:2016, a standardized protocol for the DCFH assay specifically for NMs (ISO, 2016). This ISO standard uses RAW267.4 macrophages, and in contrast with the classical assay, uses flow cytometry as read-out method.

The current study compares the classically used plate reader-based DCFH assay protocol to the ISO/TS 19006:2016 protocol (flow cytometry) in terms of reliability, sensitivity and ease of use. Additionally, pitfalls of the plate reader-based DCFH assay protocol are established and optimizations for the flow cytometry-based protocol are provided, with the aim to facilitate accurate assessment of NM-induced intracellular ROS using the DCFH assay, which can be used for hazard screening purposes in a SSbD approach.

2. Materials and methods

2.1. Chemicals

5-(and-6)-chloromethyl-2′,7′-dichlorodihydrofluorescein diacetate, acetyl ester (CM-H₂DCFDA-AE) was purchased from Invitrogen (C6827) and stored at $-20\,^{\circ}\text{C}$. This type of DCFH probe was chosen for its improved intracellular retention. CM-H₂DCFDA-AE is referred to as 'the DCFH probe' throughout the manuscript. 3-Morpholinosydnonimine hydrochloride (SIN-1) was purchased from Abcam (ab141525), dissolved in DMSO (Sigma-Aldrich, D8418) to a concentration of 100 mM, and stored at $-20\,^{\circ}\text{C}$. Diethyl Maleate was purchased from Sigma-Aldrich (D97703). Rotenone was purchased from Sigma-Aldrich (45656), dissolved in DMSO to a concentration of 100 mM and stored at $-20\,^{\circ}\text{C}$. tert-Butyl hydroperoxide (tBHP) was purchased from Sigma-Aldrich (416665).

2.2. Nanomaterials

Spherical, aminated polystyrene latex nanoparticles (60 nm, with amino surface groups) (PS-NH₂) were purchased from MagSphere (AM060NM) and stored at 4 °C. PS-NH₂ particles were delivered in a suspension in distilled water containing an unknown cationic surfactant and no sodium azide. Representative TEM images of similar 60 nm PS-NH₂ particles have been published previously (Xia et al., 2008).

Titanium dioxide (TiO_2) nanomaterials were obtained from Skyspring (7918DL). Characterisation details including a representative SEM image are available online at the supplier's website. Briefly, the particles were specified to have a diameter of 10–30 nm, a specific surface area of 50–100 m²/g and were composed of 30–40 wt% rutile and 60–70 wt% anatase crystal structures.

Nanoparticle carbon black (NPCB) (Printex-90) was obtained from Orion Engineered Carbons. The particles were characterised by the supplier to have an average diameter of 14 nm and a specific surface area of 350 $\rm m^2/\rm g$. Further characterisation details of Printex-90 including representative TEM images are widely available in literature (e.g. Saber et al., 2012 and Shen et al., 2018).

2.3. Cell culturing

The RAW264.7 murine macrophage cell line was purchased from ATCC (TIB-71). Cells were cultured using DMEM/F-12 glutamax (Gibco 31331–028) supplemented with 10% heat-inactivated fetal bovine serum, 1% Sodium Pyruvate (Gibco, 11360–070) and 1% Penicillin/ Streptomycin (Gibco, 15140–122). Treatment medium for RAW264.7 cells was phenol red free DMEM/F-12 F12 (Gibco 214041–025), without further supplementation.

A549, J774A.1 and MH-S cells were purchased from ATCC, and maintained in RPMI 1640 Medium (Gibco), 10% heat-inactivated fetal bovine serum, 100 U/mL penicillin and 100 μ g/mL streptomycin (Thermo Fisher Scientific). Treatment medium for A549, J774A.1 and MH-S cells was phenol red-free RPMI, with added FBS, and without further supplementation.

Cells were cultivated at 37 $^{\circ}\text{C}$ and 5% $\text{CO}_2,$ and discarded by passage 20.

2.4. Characterisation of PS-NH₂

2.4.1. Dynamic light scattering

Size distribution, zeta potential, and polydispersity were assessed using dynamic light scattering (DLS) in water and in treatment medium. Size and zeta potential measurements were carried out on three individual samples, in three technical replicates (Using Malvern Zetasizer Ultra).

2.4.2. Determination of delivered dose to cells

Effective density was determined as described in Deloid et al. (DeLoid et al., 2017). Briefly, dispersions of 10 $\mu g/mL$ of PS-NH $_2$ were made in treatment medium. The samples were centrifuged for 1 h at 3000 xg in Packed Cell Volume (PCV) tubes (TPP, Z760986) in a swing-out rotor, and pellet size was derived using an easy read measuring device (TPP, 87008). No pellet was visible, therefore it was assumed that effective density was equal to material density. The dose delivered to cells was modelled using the DG model in the DosiGUI software (last updated 12/11/2021, and developed in MATLAB R2020b) (Botte et al., 2021). The following inputs were used:

- Solvent dynamic viscosity: 0.00073 Pa·s.
- Medium density: 0.9999 g/mL.
- Material density & Effective density: 1.055 g/mL.
- Stickiness: Assumed high due to positive charge of PS-NH2.

Additionally, the dimensions of 24-wells plate wells and the sizedistributions resulting from DLS measurements were used.

2.5. Testing acellular reactions of test compounds with CM-H₂DCFDA-AE

The NanoGenotox dispersion protocol (Jensen, 2018) was followed to make dispersions of all NMs for this experiment, to avoid an effect of sonication duration on the direct reactions with CM-H₂DCFDA-AE (DCFH probe). In short, NM powders were prewetted with 0.5% EtOH, after which MQ was added and probe sonication was applied for 16 min at 10% amplitude. The addition of BSA was omitted to avoid an effect on direct reactions. Dispersions of PS-NH₂ were made by directly diluting in treatment medium, as they are already in suspension and do not require sonication. Soluble chemicals were directly diluted in treatment medium. The medium used for this experiment was RAW264.7 treatment medium (phenol-red free and FBS-free DMEM/F-12).

DCFH probe was dissolved in DMSO and diluted to a concentration of 6 $\mu g/mL$ in HBSS (Gibco, 14175–053). DCFH probe diluted in HBSS, or HBSS alone, was added to the wells of a black 96-wells plate (100 μl per well). An equal volume of test substance diluted in treatment medium was added to the wells. Plates were incubated at 37 $^{\circ}$ C in the dark, and fluorescence was measured at time points 2, 4, 6, and 24 h using a Spectramax M2 plate reader. Excitation and emission wavelengths of ex495/em525 nm were used for all acellular experiments, unless stated otherwise. The background signal of NMs in HBSS was subtracted from the fluorescence.

2.6. Classical plate reader-based DCFH assay protocol

For the plate reader-based protocol, RAW264.7 cells were seeded on black 96-wells plates with flat transparent bottom at a density of 1.5 \times 10⁵ cells/cm². They were then allowed to settle and attach overnight at 37 °C and 5% CO_2 to reach $\pm 80\%$ confluency. On day two, DCFH probe was prepared by dissolving it in DMSO and subsequent dilution in treatment medium to a concentration of 6 µg/mL and kept in the dark. Cells were washed gently with pre-warmed (37 °C) HBSS (Gibco, 14175-053) by pipetting and gentle aspiration. They were then incubated with DCFH probe at 100 μ l/well for 30 min at 37 °C and 5% CO₂. After incubation, cells were washed twice and treatments (prepared in treatment medium) were applied. After 24 h, fluorescence was measured using a Spectramax M2 spectrophotometer. Fluorescence was measured again after gently washing cells once with pre-warmed (37 °C) HBSS and applying fresh HBSS. Excitation and emission wavelengths of ex485/ em520 nm were used for all cellular experiments, unless stated otherwise. Gain was set to high for all experiments. For an overview of the protocol, see Fig. 1.

2.7. Fluorescence microscopy

For fluorescence microscopy analysis the classical DCFH assay protocol was followed, but instead of using a plate reader, the Leica DMI4000 B Inverted Microscope and DFC450C camera were used. The cells were imaged directly in the plate in phenol red-free medium after washing (no fixation) at 200× magnification. The FITC channel was used for fluorescence imaging with constant 1 s exposure time and $1\times$ gain.

2.8. Testing DCFH translocation from cells to supernatant

2.8.1. RAW264.7

The plate reader-based DCFH protocol (see above) was followed for seeding RAW264.7 cells and probing with DCFH probe. On day 2, the cells were not exposed to NMs or other treatments. Instead, supernatant from the cells was collected at time points: 0, 2, 4, 6, and 24 h after the DCFH incubation step, and was stored at 4 $^{\circ}$ C, protected from light. After

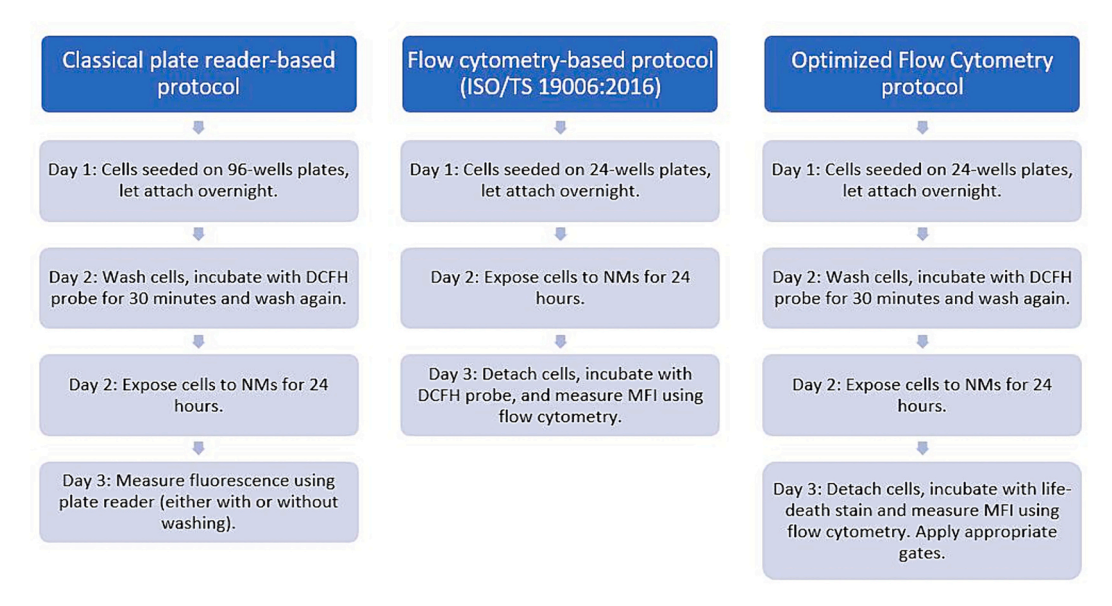


Fig. 1. Overview of protocols. The plate reader-based protocol is also commonly performed with the DCFH probe incubation after exposure to the NMs. In this current paper, this approach was not used.

the collection of the 24-h time point, a $1\%~H_2O_2$ solution in MQ water was added to the supernatants to visualize the DCFH present in the supernatant. As a background control, $1\%~H_2O_2$ solution in cell culture medium was used. H_2O_2 and supernatants were incubated for 3~h at $37~^\circ\text{C}$, and then centrifuged for 10~min at 1000~xg to get rid of cell debris that might cause autofluorescence. Supernatants were then transferred to black 96-wells plates and fluorescence was measured. Log2 fold change as compared to the negative control was calculated.

2.8.2. A549, J774A.1 and MH-S cells

This experiment aimed to confirm translocation from cells other than RAW264.7. A549, J774A.1 and MH-S cells were seeded on 96-well plates at a density of 2×10^5 cells/cm 2 . Cells were then allowed to settle and attach overnight at 37 $^{\circ}\text{C}$ and 5% CO_2 to reach near-confluency to avoid surface area gaps and loss of fluorescent signal due to lack of cells present. The plate reader-based DCFH protocol (see above) was followed for DCFH probe incubations and washes. After probing, the cells were treated with tert-Butyl hydroperoxide (tBHP) diluted in phenol red-free treatment medium, supplemented with 10% FBS. After 90 min, fluorescence was measured on plate reader at wavelengths ex495/em525, after which supernatant was collected and cells were washed and both were measured again separately.

2.8.3. LC-MS analysis

Cell culture medium samples from the 2-h timepoint of the RAW264.7 translocation experiment were analysed using liquid chromatography high resolution mass spectrometry (LC-HRMS), after centrifugation. The sample volume was transferred to an amber HPLC vial prior to the analysis. The LC-HRMS system consisted of a Thermo Fisher Scientific Vanquish UPLC (quaternary pump, degasser, autosampler, and column oven) coupled to a Thermo Fisher Scientific Exploris120 mass spectrometer equipped with a heated electro spray probe. The LC separation was performed on an Accucore UPLC reversed phase column (Phenyl Hexyl $2.6\,\mu m$ $2.1\, imes\,100\,mm$). Mobile phase consisted of 10 mM ammonium formate in water (Mobile phase A) and 10 mM ammonium formate in acetonitrile:methanol 1:1 v/v (mobile phase B). A volume of 10 µl of cell culture medium was injected. A gradient was performed, starting with 1% mobile phase B, held for 1 min followed by an increase to 99% from 1 to 10 min, where the concentration of mobile phase B 99% was held for an additional 1.5 min. After

which it was returned to the initial conditions and re-equilibrated for 4.5 min prior to the next injection cycle.

MS data acquisition was performed using data dependent fragmentation in both positive and negative mode. With a full scan m/z range from 100 to 1000 with a resolution of 60000 followed by 4 data dependent fragmentations for negative mode with a resolution of 15000, and 2 data dependent fragmentations in positive mode. Precursor ions observed in negative mode are reported. The analysis was carried out on three independent experiments, each containing two technical replicates. Results from one experiment are shown, but results were consistent across repeats.

2.9. Optimized flow cytometry-based DCFH protocol

For the optimized flow cytometry-based measurements, the ISO standard ISO/TS 19006:2016 was followed with some modifications. The complete SOP can be found in Supplemental materials 1, and an overview of the SOP in Fig. 1. In short, RAW264.7 cells were seeded on a 24-wells plate at a density of 1×10^5 cells/cm² (slightly more than suggested in ISO standard). They were then left to settle and attach overnight at 37 °C and 5% CO2 to reach 80% confluency. On day 2, DCFH probe was prepared by dissolving in DMSO and subsequent dilution in treatment medium to a concentration of 6 µg/mL, and kept in the dark. Cells were washed gently with pre-warmed (37 °C) HBSS by pipetting and gentle aspiration. They were then incubated with DCFH probe at 250 µl/well for 30 min at 37 °C and 5% CO₂. After incubation, cells were washed twice again and treatments (prepared in treatment medium) were applied at 500 µl per well. PS-NH2 was directly diluted in treatment medium without sonication. Agglomeration of the stock dispersion of PS-NH2 was monitored closely using DLS. After 24 h, supernatant was collected and cells were detached by gentle scraping (using Mini Cell Scrapers (Biotium, 22003)), pipetting and washing with HBSS. Supernatant and cells were combined in 15 mL tubes and centrifuged at 400 xg for 5 min. Live-death stain (Fixable viability stain 780, BD Bioscience 565388) was diluted 1:1000 in cold HBSS. After centrifugation, supernatant was discarded, pellets were resuspended in $200\,\mu l$ live-death stain and incubated for 20 min at 4 $^{\circ} C$ in the dark. Cells were washed and centrifuged at 400 xg for 5 min once more and pellets were resuspended in cold HBSS and transferred to FACS tubes (Falcon, 352008) with lid (Falcon, 352032) on ice. Flow cytometry analysis was

carried out immediately afterwards using BD Biosciences Fortessa Cell Analyzer. Singlets and alive cells were gated for using the APC-Cy7 channel and median fluorescence intensity for DCF was recorded using FITC channel. 10.000 events were collected within the alive gate. Settings were kept constant for all analyses.

2.10. Comparison between flow cytometry and plate reader-based measurements

For the comparison between flow cytometry and plate reader, the optimized flow cytometry-based protocol was followed, and cells were split up between FACS tubes and black clear bottom 96-wells plates. FACS tubes were analysed as described above. Cell density in 96-well plates was confirmed to be sufficient (covering the entire bottom of the well, no gaps) by microscopy and measured using the plate reader, with gain set to high.

2.11. Sensitivity measurements of plate readers

The comparison between flow cytometry and plate reader was carried out in two separate labs. Therefore, both plate readers were tested for their sensitivity. Fluorescein diacetate (F-DA) (Sigma F7378) was dissolved in acetone in two steps to reach a 1 mM F-DA solution. F-DA was activated by adding 0.01 M NaOH to reach a concentration of 200 μ M F-DA, which was incubated for 5 min at RT in the dark. This solution was diluted to 50 μ M in PBS and then diluted to the top standard concentration of 0.5 μ M. In a black, clear-bottomed 96-wells plate serial dilutions of 1:1 were made for a total of 15 concentrations. The lowest concentration tested was 0.038 nM, and PBS alone was included as 0 nM. Fluorescence was measured at wavelength ex485/em520 nm. The spectrophotometer used in lab 1 was a Spectramax M2 and in lab 2 a Varioskan LUX. The gain was set to high in both spectrophotometers.

2.12. Optimized flow cytometry-based protocol with inverted incubation

To make the comparison between probing with DCFH before and probing after NM exposure, incubation with DCFH probe was performed after treatment of the cells. The optimized flow cytometry-based protocol was followed, except: On day 2, treatments prepared in treatment medium were added at 500 μ l per well. On day 3, DCFH probe was prepared by dissolving in DMSO and subsequent dilution in treatment medium to a concentration of 6 μ g/mL and kept in the dark. After 24 h of incubation with the NM treatments, supernatant was collected and cells were detached by gentle scraping (using Mini Cell Scrapers (Biotium, 22,003)), pipetting and washing with pre-warmed (37 $^{\circ}$ C) HBSS. Supernatant and cells were combined in 15 mL tubes and centrifuged at 400 xg for 5 min. Cells were then resuspended in the prepared DCFH probe solution at 250 μ l/tube for 30 min at 37 $^{\circ}$ C and 5% CO₂. Cells were centrifuged at 400 xg for 5 min, after which the optimized protocol was followed for life-death stain incubation and flow cytometry analysis.

2.13. Data analysis

Each individual experiment was carried out a minimum of three times, each containing at least two technical replicates for flow cytometry analysis and three technical replicates for plate reader analysis. Normal distribution of data was assumed, and therefore averages of each biological replicate were analysed by one-way ANOVA, followed by Dunnett's multiple comparisons test, using GraphPad Prism version

9.5.1. For Fold-change or Log2 Fold-change data, unpaired t-tests were performed to compare two treatments.

3. Results

3.1. NM characterizations

Characterizations of NMs tested in the cellular experiments are depicted in Table 1. The deposited doses as calculated using the DG model are shown in Supplementary Table S1 (Supplementary materials 2)

3.2. In-depth evaluation of the plate reader-based protocol

Several pitfalls of the classical plate reader-based protocol related to instability of 5-(6)-Chloromethyl-2',7'-dichlorodihydrofluorescein diacetate acetyl ester (CM-H $_2$ DCFDA-AE, referred to as DCFH probe), translocation of DCFH metabolic products from cells to supernatant, and lack of sensitivity of spectrophotometry measurements are shown in this section.

3.2.1. Acellular reactions of DCFH probe with chemicals and NMs

Fig. 2 shows that incubation of the DCFH probe with several commonly used positive controls and NMs in an acellular environment leads to a substantial amount of fluorescence, in a time-dependent manner.

3.2.2. DCFH translocation from RAW264.7 cells to the supernatant

Fig. 3 shows that DCFH is released from the cells into the supernatant in a time-dependent manner. RAW264.7 cells were incubated with DCFH probe, and washed thoroughly before being put on clean serum-free medium. At each time point, supernatant was collected, and all

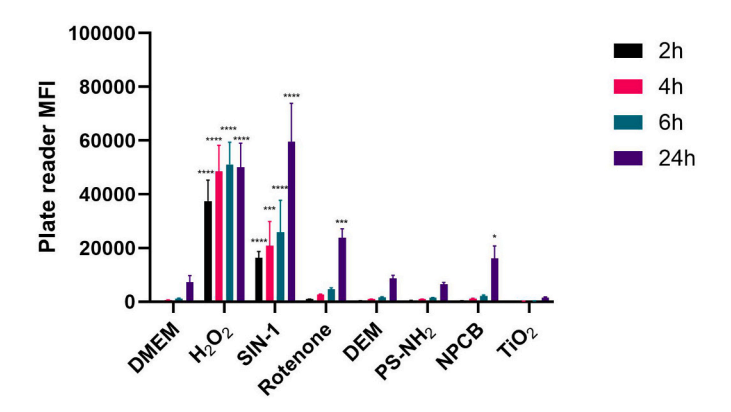


Fig. 2. Acellular reactions of CM-H₂DCFDA-AE with several commonly used positive controls and nanomaterials. DMEM = DMEM/F-12 without phenol red and without serum. H₂O₂ = 1% Hydrogen Peroxide in DMEM. SIN-1 = 100 μ M SIN-1 in DMEM. Rotenone = 50 μ M in DMEM. DEM = 50 μ M Diethyl Maleate in DMEM. PS-NH₂ = 10 μ g/mL aminated polystyrene nanoparticles (60 nm) in DMEM. NPCB = 10 μ g/mL nanoparticle carbon black in DMEM. TiO₂ = 100 μ g/mL anatase/rutile titanium oxide nanoparticles (10–30 nm) in DMEM. TiO₂, NPCB and PS-NH₂ results were corrected for possible autofluorescence. MFI = mean fluorescence intensity. *p < 0.05, **p < 0.01, ***p < 0.001, ****p < 0.0001 as determined by one-way ANOVA compared to the DMEM 2 h condition. (For interpretation of the references to colour in this figure legend, the reader is referred to the web version of this article.)

Table 1
DLS analysis of aminated polystyrene NMs (PS-NH₂) in DMEM/F-12 treatment medium and water, performed directly after making dispersions (10 μg/mL).

NM	Medium	Z-average (nm)	Zeta potential (mV)	Polydispersity index	Effective density (g/cm ³)
PS-NH ₂	Water	60.8 ± 0.8	46.39 ± 4.69	0.021 ± 0.011	N/A
PS-NH ₂	DMEM/F-12 treatment medium	569.9 ± 124.3	-4.20 ± 9.83	0.219 ± 0.032	1.055

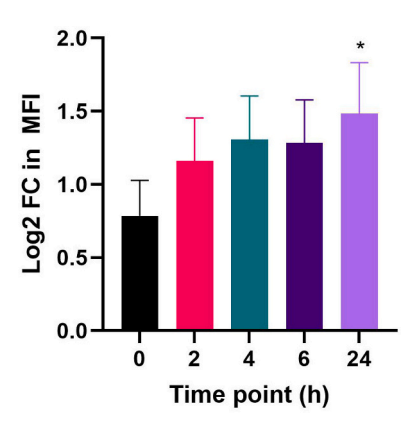


Fig. 3. Translocation of DCFH from RAW264.7 cells into the supernatant over time, visualized by its direct reaction with $\rm H_2O_2$ after supernatant collection. Results are depicted in Log2 fold-change in fluorescence as compared to the background control ($\rm H_2O_2$ in medium). MFI = mean fluorescence intensity. *p < 0.05 as determined by one-way ANOVA compared to 0 h time point.

supernatants were incubated with hydrogen peroxide at the 24-h time-point in order to induce fluorescence to quantify the amount of reagent that had translocated into the medium. The results (Fig. 3) show an increase in fluorescence of up to $3\times$ (Log2: $1.5\times$) as compared to the background control after 24 h of incubation. The mechanism behind this translocation is unknown, and can be either active or passive.

3.2.3. Effect seen on plate reader is mostly due to fluorescent supernatant of A549, J774A .1 and MH-S cells

The translocation of CM- $\rm H_2DCFDA$ -AE metabolic products to the supernatant in other cell types was confirmed in a second laboratory using A549, J774 A.1, and MH-S cells (Fig. 4). Cells were incubated with DCFH probe, washed, and treated with tert-butyl hydroperoxide (tBHP). After 90 min, plates were analysed on a plate reader, after which supernatant was collected, and washed cells and supernatant were measured separately. The whole measured effect could be attributed to the supernatant's fluorescence, with no observed signal increase in the cells alone.

3.2.4. Identification of DCFH products in cell culture supernatant

Samples from the 2-h timepoint were analysed using Liquid chromatography/mass spectrometry (LC-MS) to identify the components that had translocated from the cells into the supernatant. Quantitative values could not be estimated as stable and pure calibration curves of DCF and H_2DCF could not be established. The intensity of DCF and H_2DCF detected in the cell supernatant by LC-MS was low and close to the detection limit. A total of five metabolic products of the original CM- H_2DCFDA -AE reagent were detected in the supernatant, of which H_2DCF and DCF in the highest relative quantities (Fig. 5). The translocation of H_2DCF to the extracellular compartment is of particular relevance for the plate reader-based protocol, as it is capable of reacting with positive control chemicals or particles to form the fluorescent DCF. Molecular structures, molecular weights and molecule formulas can be found in Supplementary Fig. S1 (Supplementary materials 2).

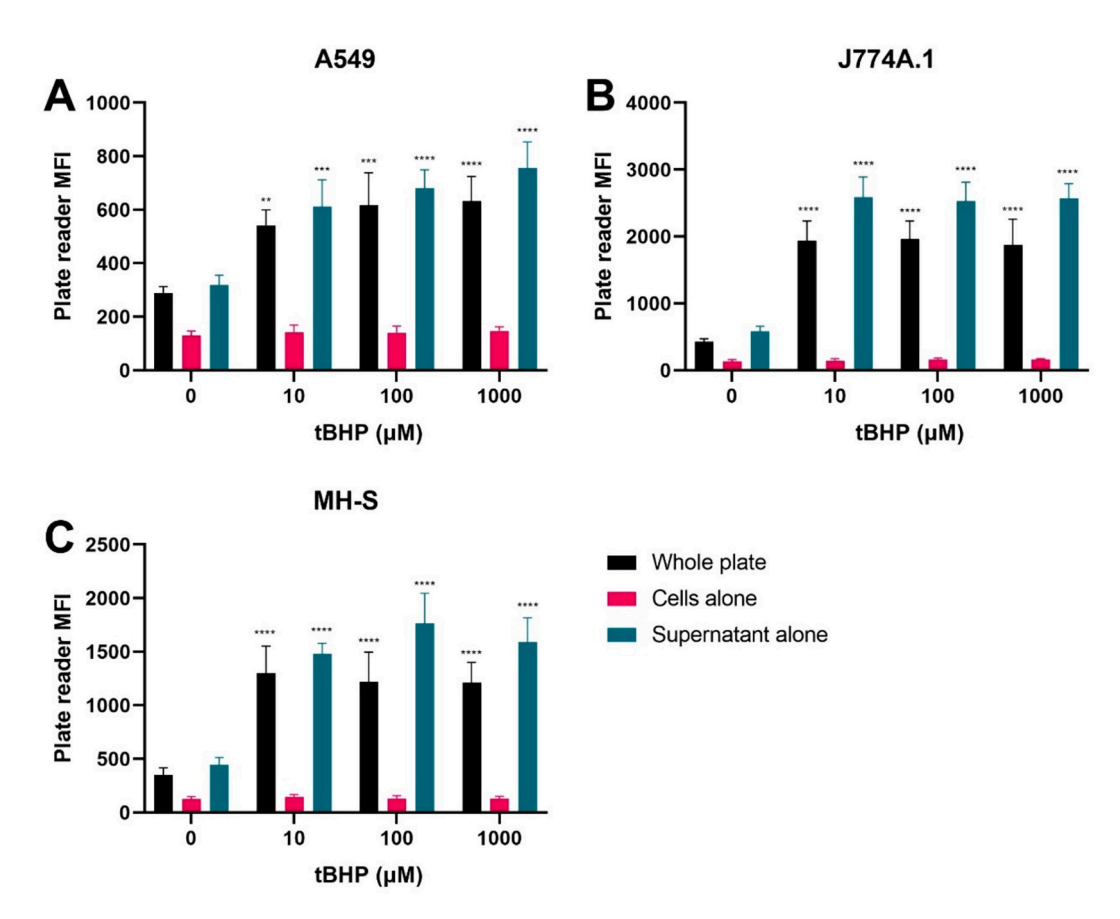


Fig. 4. Fluorescence intensity in wells, in washed cells alone, and in supernatant alone after performing the classical plate reader-based DCFH assay protocol. Cell types: 4A: A549, 4B: J774A.1, 4C: MH-S. Results were obtained after 90 min of incubation with tBHP. MFI = mean fluorescence intensity. *p < 0.05, **p < 0.01, ***p < 0.001, ****p < 0.0001 as determined by one-way ANOVA compared to respective medium only condition.

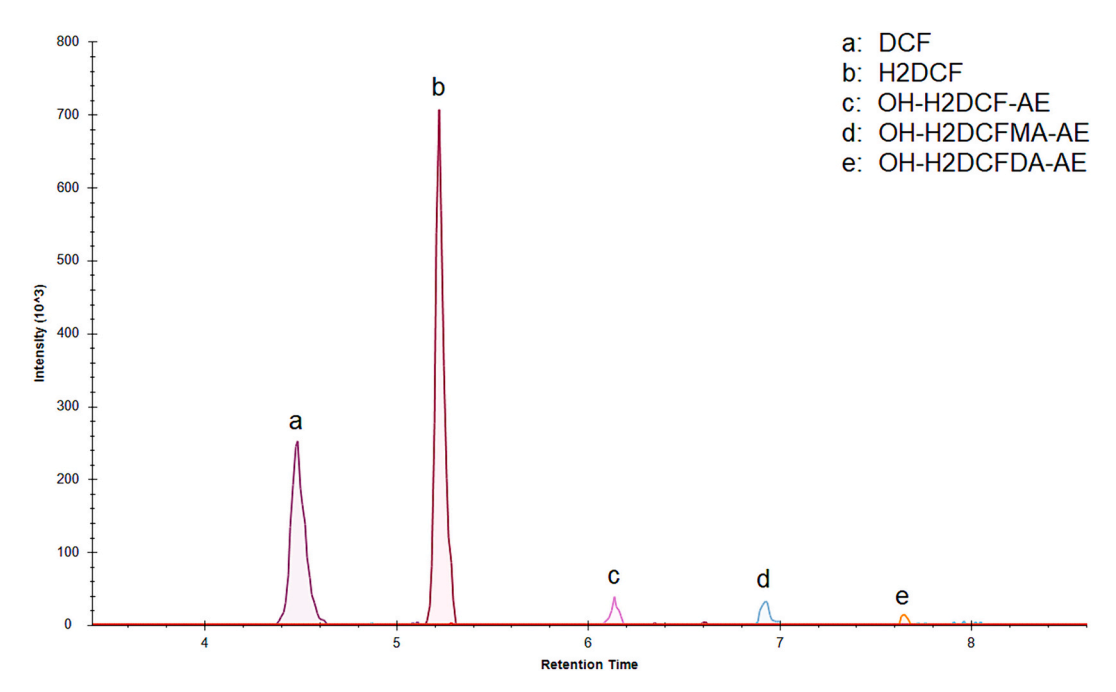


Fig. 5. LC-MS chromatogram of cell culture supernatant of RAW264.7 cells collected two hours after incubating with the DCFH probe. Five metabolic products of the original DCFH probe CM-H₂DCFDA-AE were detected.

3.3. Optimizing ISO/TS 19006:2016

The ISO standard ISO/TS 19006:2016 (ISO, 2016) uses flow cytometry as read-out method instead of a plate reader. Possible improvements of the ISO protocol related to the timing of DCFH probe incubation, and to proper gating of cell populations are shown in this section using aminated polystyrene NMs (60 nm) (PS-NH₂), which are suggested as a positive particle control by the ISO standard.

3.3.1. Incubation with DCFH probe before exposure to NMs gives a more reliable and sensitive response

We compared incubating cells with DCFH probe before and after exposure to the NMs. Incubation with DCFH probe after exposure to the NMs gives a much higher, yet more variable fluorescent signal as compared to incubating before exposure (Fig. 6A). However, when expressed as fold change of the signal (Fig. 6B), DCFH probe incubation before exposure to the NMs gives a higher response compared to incubation afterwards, suggesting a cumulative working mechanism of the DCFH probe. This means that the DCFH probe is likely able to detect all

ROS it encounters during 24 h, and remains fluorescent long enough to determine the cumulative amount of ROS during this time. Analysis of cell viability in the before *vs* after group showed no difference in cell viability (negative control showed 92.6% viability in before group, and 91.1% viability in after group).

3.3.2. Technical guidance on flow cytometry sample and data processing improves the reliability of the protocol

The ISO standard does not specify any guidelines on gating strategies and how to properly analyze results. In Fig. 7, we show how this approach may lead to an overestimation of the effect as compared to when a proper gating strategy is followed. The flow cytometry-based protocol was carried out on RAW264.7 macrophages treated with PS-NH $_2$ and results were analysed in two different ways:

- 1) Following ISO/TS 19006:2016: No gating specified
- 2) Following a gating strategy: singlet gating and live cell-gating (using live-death stain)

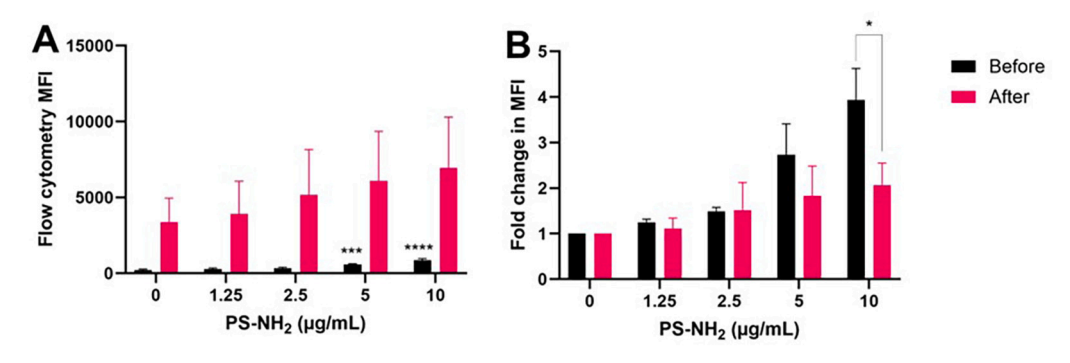


Fig. 6. Comparison of the flow cytometry-based protocol using probing before incubation with the treatment versus after. MFI= median fluorescence intensity. 6A: Results expressed as absolute MFI. 6B: Results expressed as fold change in MFI as compared to the negative control. *p < 0.05, **p < 0.01, ***p < 0.001, ****p < 0.001 as determined by one-way ANOVA compared to respective medium only condition (5A) or by unpaired t-test comparing the before and after condition of each concentration (5B).

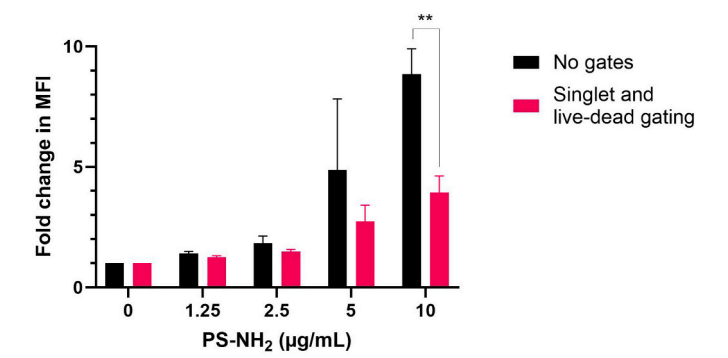


Fig. 7. The DCFH assay carried out using flow cytometry as read-out, showing the difference in fold change in fluorescence between the analysis suggested in the ISO standard *versus* using a gating strategy including singlets gating and live-dead staining. MFI = median fluorescence intensity. $^{**}p < 0.01$ as determined by unpaired t-test comparing the no-gates and gates condition of each concentration.

An overestimation of 2.2-fold can be seen in Fig. 7 when no gates are applied in flow cytometry analysis. The overestimation is already reduced to 1.14-fold upon applying a singlets gate only, which automatically gates out debris, suggesting that the overestimation results from auto-fluorescent cell debris and remaining NMs.

3.3.3. SIN-1 is not a suitable positive control for the DCFH cellular assay ISO/TS 19006:2016 suggests the use of SIN-1 at a concentration of 5 μM as a chemical positive control. Using the plate reader-based protocol without washing before measuring, SIN-1 gives a 4-fold increase in fluorescent signal (Fig. 8). When analysing cells exposed to SIN-1 using flow cytometry, a response is only seen at 100 μM , and no clear doseresponse pattern is observed. This suggests direct reactivity of SIN-1 with the DCFH probe molecule (as was also found after direct incubation as shown in Fig. 2), and very little intracellular ROS formation.

3.4. Comparison between plate reader, flow cytometry, and microscopy

Here, the plate reader-based protocol is compared to the optimized flow cytometry protocol, as described in detail in the methods section. The most important optimizations to the ISO standard are:

- 1. Incubation with CM-H $_2\mbox{DCFDA-AE}$ before exposure, instead of after exposure
- 2. Using an appropriate gating strategy

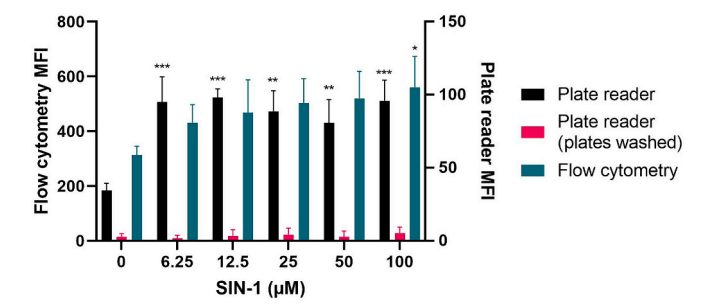


Fig. 8. DCFH assay with SIN-1 carried out using the plate reader-based protocol (with and without washing before measuring) and the optimized flow cytometry-based protocol. Results are expressed as median fluorescence intensity (MFI) for flow cytometry and mean fluorescence intensity (MFI) for plate reader-based measurements. $^*p < 0.05$, $^{**}p < 0.01$, $^{***}p < 0.001$ as determined by one-way ANOVA compared to respective medium only condition.

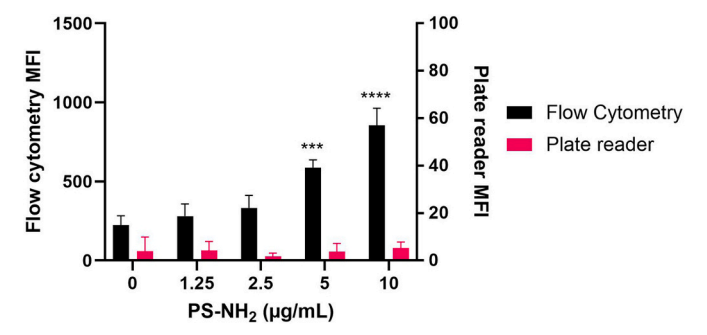


Fig. 9. Direct comparison of the plate reader-based protocol (with washing) with the optimized flow cytometry-based protocol in RAW264.7 cells in response to PS-NH₂. Results are expressed as median fluorescence intensity (MFI) for flow cytometry and mean fluorescence intensity (MFI) for plate reader-based measurements. ***p < 0.001, ****p < 0.0001 as determined by one-way ANOVA compared to respective medium only condition.

A direct comparison of the plate reader-based protocol (with washing before measurement) with the optimized flow cytometry protocol is shown in Fig. 9. The results obtained with the plate reader-based protocol correlate poorly with the fluorescence observed using the optimized flow cytometry-based protocol.

Plate reader-obtained values also correlate poorly with what was observed using fluorescence microscopy (Fig. 10). To obtain the microscopy pictures shown in Fig. 10, the original plate reader-based protocol was followed, but cells were analysed using fluorescence microscopy instead of plate reader. Fluorescence was not quantified, but the increase in intracellular fluorescence in the PS-NH₂ treated cells as compared to the negative control can be easily appreciated.

A direct comparison between flow cytometry and plate reader was performed by dissociating and dividing cells between 96-wells plates and flow cytometry tubes. This comparison was carried out in two different laboratories, and allows for the direct comparison of sensitivity of the two read-out methods on exactly the same cell samples. It was ensured that the lack in sensitivity of the plate reader was not due to a low cell density by transferring cells to the plates at a high enough density to ensure coverage of the entire well bottom, Fig. 11A&B (lab 1) and Fig. 11C&D (lab 2) show the increased sensitivity of flow cytometry over plate reader analysis. To verify and quantify the sensitivity of both plate readers, a standard concentration range of fluorescein was measured in both plate readers, and results are shown in Supplementary Fig. S2 (Supplementary materials 2). Although the standard curves show considerable differences in the detection of fluorescence at higher concentrations of fluorescein, the limit of detection was satisfactory for both plate readers (significant increase in fluorescence from 78.3 nM fluorescein in lab 1, and 19.6 nM fluorescein in lab 2).

4. Discussion

The cellular DCFH assay is widely used and at the same time widely discussed in literature (Aranda et al., 2013; Kroll et al., 2012; Pal et al., 2014; Wang and Joseph, 1999). The assay was considered especially useful as oxidative stress could be assessed at multiple time-points, without the need to wash away the treatment (Wan et al., 1993; Wang and Joseph, 1999). In this paper we present several caveats that are in contrast with previously established benefits of the assay, and we propose critical optimizations. The recommendations discussed here may help future researchers carry out the assay as accurately as possible.

4.1. Plate reader-based measurements

4.1.1. Translocation of DCFH from cells to supernatant

We have shown that five metabolic products of the DCFH probe appear extracellularly in the supernatant of RAW264.7 cells, and that

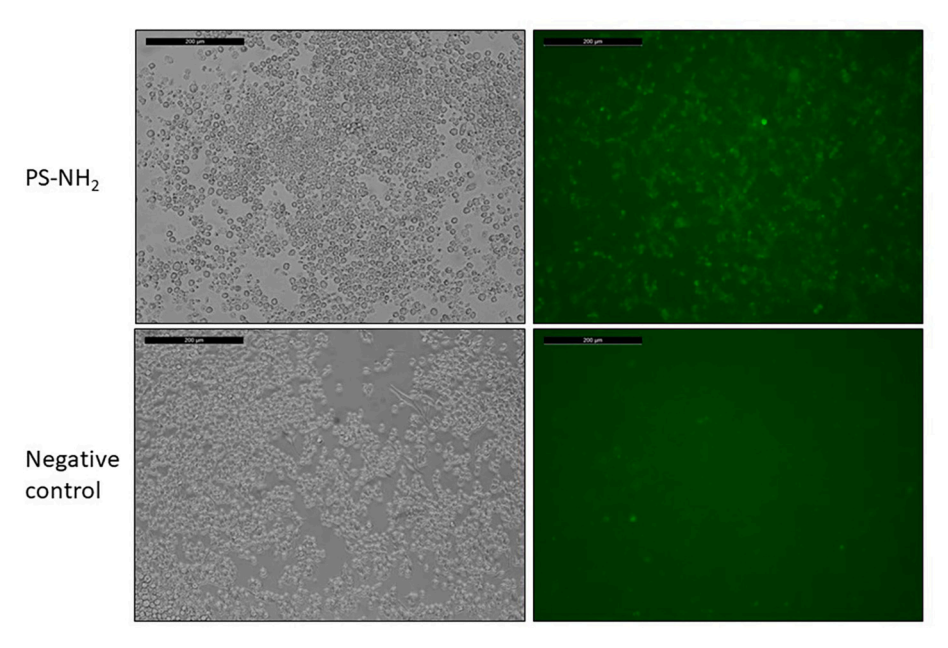


Fig. 10. Fluorescence microscopy showing visibility of fluorescence in RAW264.7 cells after treatment with $10 \mu g/mL$ PS-NH₂. The classical plate reader-based protocol was followed for the probing and exposures of the cells, and cells were washed before imaging. Scale bar = $200 \mu m$. Magnification = $200 \times$.

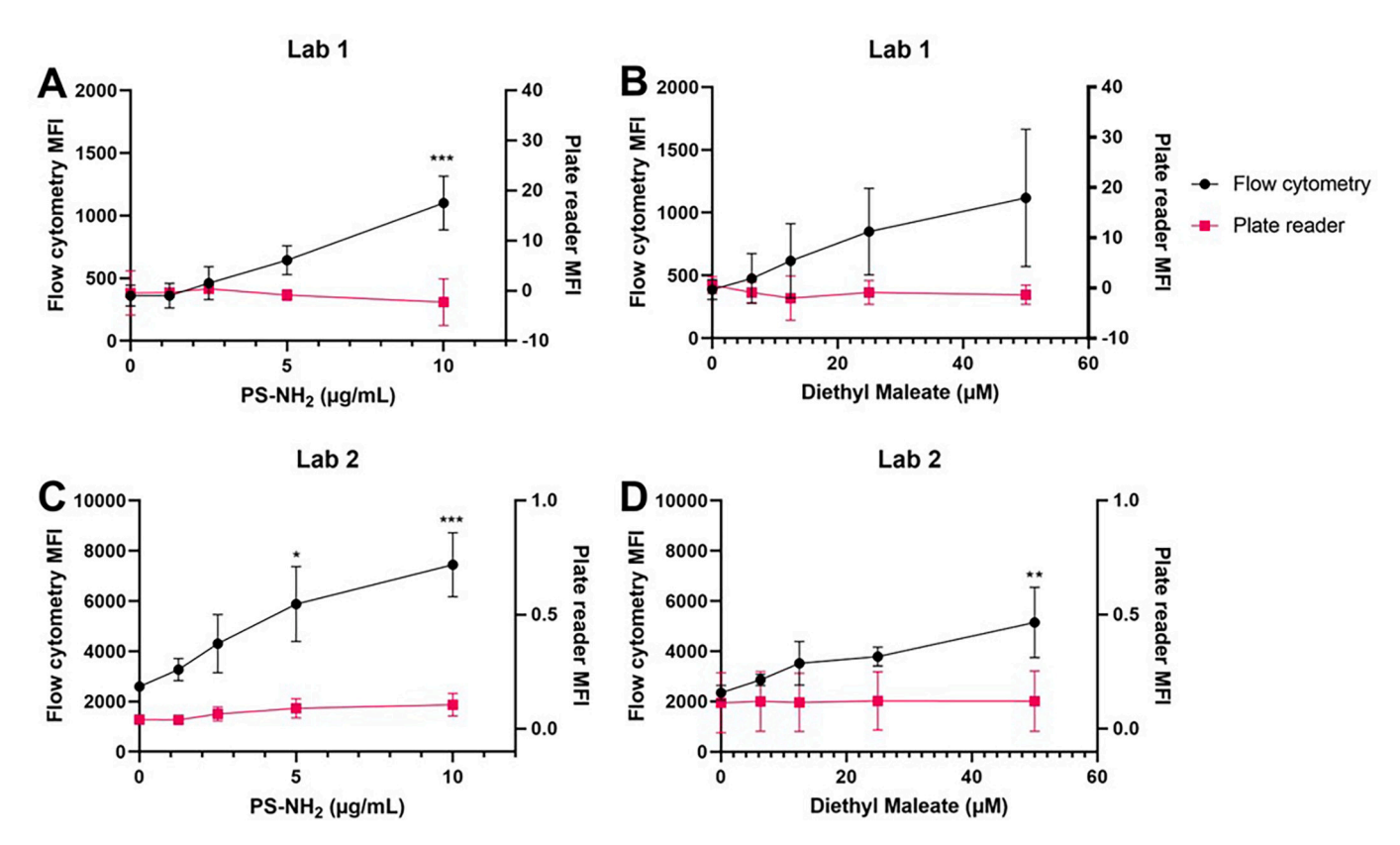


Fig. 11. Flow cytometry and plate reader analysis carried out on the same cell sample. The optimized flow cytometry-based protocol was followed. 11A & 11B were carried out in lab 1. 11C & 11D were carried out in lab 2. Results are expressed as median fluorescence intensity (MFI) for flow cytometry and mean fluorescence intensity (MFI) for plate reader-based measurements. *p < 0.05, **p < 0.01, ***p < 0.01 as determined by one-way ANOVA compared to respective medium only condition.

extracellular fluorescence is a concern in A549, J774A1, and MH-S cells as well. The increase in fluorescent signal in response to positive controls measured using a plate reader can be largely attributed to the fluorescence of the supernatant, from an already fluorescent form released from the cell combined with a non-oxidized form which is subsequently

oxidized externally. For these experiments, CM- H_2 DCFDA-AE was used, known for its better cellular retention due to its ability to form covalent bonds with intracellular components by replacing the chlorine in its chloromethyl (CM) group by the thiolgroup belong to a cellular component.

Release of DCF from cells has been described before and in itself does not pose a large issue for the assay, as the extracellular fluorescence should be representative of intracellular ROS, or can easily be corrected for (Reiniers et al., 2021). However, the relatively large quantities of the non-fluorescent $\rm H_2DCF$ that were detected in the cell supernatant are available to react with the exposure treatments present in the cell culture medium, leading to a false positive of an assumed cellular reaction. Although washing before plate reader-based measurements may help circumvent this issue, concerns about method sensitivity remain.

4.1.2. Sensitivity

Lack of sensitivity of plate reader-based intracellular fluorescence measurements has previously been described in literature, for example for calcium detecting dyes (Heusinkveld and Westerink, 2011), and is confirmed here by comparing plate reader to flow cytometric, and fluorescence microscopy outcomes. Quantitative outcomes of the plate reader do not match the intracellular fluorescence quantified using flow cytometry and qualitatively observed using fluorescence microscopy.

In order to reduce interference by NMs, thorough washing is required prior to measuring. Washing is also performed before incubation with DCFH probe, and twice afterwards, which could lead to loss of cells. When cells were transferred to new 96-wells plates at a density ensuring total coverage of the well bottom, plate reader sensitivity was still not satisfactory, whereas plate readers were sensitive enough to detect low amounts of fluorescein. It should be noted that for the cellular measurements, 24-h incubations were performed, which will have caused the fluorescence intensity to have faded.

4.1.3. Direct reactions

We confirmed the possibility of direct reactions of NMs with DCFH probe outside of the cell as previously suggested (Kroll et al., 2011; Kroll et al., 2012). CM-H₂DCFDA-AE showed substantial direct reactions with several commonly used positive controls and NMs in an acellular environment, whereas it should become responsive to ROS only after conversion by intracellular esterases. These direct reactions of compounds with DCFH probe will have little to no implications for the cellular assay as long as flow cytometry is used, which measures intracellular fluorescence.

4.1.4. Consequences

Altogether, the current results indicate that the plate reader-based protocol warrants caution in terms of experimental setup and data interpretation. The incorrect use and interpretation of the cellular DCFH assay may have led to uncertain results in previous research. For example, in Braakhuis et al. (2016) the DCFH assay is used in a plate reader-based format, measuring fluorescence of cells exposed to Ag NMs at several time-points (Braakhuis et al., 2016). In this paper, DCFH probe (the H₂DCFDA form in this case) was added first and after a washing step Ag NMs were added. Subsequently, ROS formation was measured over time without washing. A doubling of the fluorescent signal was observed when exposed to Ag NMs, and a 20-fold increase in fluorescence was observed when exposed to the positive control H₂O₂. This measured effect is likely the result of a translocation of intracellularly oxidized DCF to the supernatant, and by a direct reaction between released H₂DCF and Ag NMs, not reflecting intracellular ROS. Although washing the cells within the plate reader format will ensure these possible false positive effects do not occur, the reduced sensitivity of the plate reader method provides incentive to quantify intracellular ROS using fluorescence microscopy, as performed in (Wang et al., 2019), or flow cytometry following the presented optimized protocol.

4.2. Flow cytometry-based measurements

4.2.1. Advantages of flow cytometry

The main advantage of the ISO standard (ISO, 2016) is the use of flow cytometry, and with this analysis at a single cell level, which showed a

much greater sensitivity as compared to plate reader-based measurements. This assay captures the events taking place intracellularly, and fluorescent supernatant as a result H₂DCF or DCF release does not pose any issues. Interference by NMs will be less significant, as agglomerates or aggregates of particles in the supernatant that are large enough to be counted as events can be gated out based on differences in morphology and granularity, leaving only the negligible interference of intracellular NMs (Guadagnini et al., 2015).

Cell loss due to vigorous washing, or unpopulated areas of cell culture plates, are also not an issue for measurements by flow cytometry, as less washing is needed, and all cells (both adherent and non-adherent) are collected for flow cytometry analysis. For some NMs, uptake can be quantified by using side scatter, as demonstrated for TiO₂ (Suzuki et al., 2007; Vranic et al., 2017), which is another highly relevant variable to evaluate in *in vitro* experiments.

Important advice given in the ISO standard is to express the fluorescence signal as fold change increase relative to the negative control. Expressing results as absolute fluorescence will create large variation between repeats, due to effects which can vary largely between days, such as photo-oxidation, photo-bleaching (Zhang and Gao, 2015), nonspecific enzymatic oxidation (Bass et al., 1983), and oxidation by haemoproteins and haem (Ohashi et al., 2002). The increase of the fluorescent signal compared to the negative control is therefore of more interest than the absolute amounts.

The ISO standard states that an incubation time of the cells with NMs of 6 and 24 h should be used. In this paper, an incubation time of 24 h was used. This is largely because previous research had shown that extending the incubation time to 24 h increases the sensitivity of the DCFH assay (Aranda et al., 2013). On the contrary, agglomeration of NMs increases over time, and agglomerated NMs exhibit enhanced interference (Aranda et al., 2013).

4.2.2. Recommendations for using flow cytometry

Although it being a step in the right direction towards more standardized methods optimized for NMs, ISO/TS 19006:2016 is not yet optimal. Incubating with DCFH probe before exposure to NMs results in a lower absolute fluorescent signal, yet it greatly increases the fold change of the effect. DCF seems to remain fluorescent for sufficiently long enough, and in order to capture all oxidative stress within a certain timeframe, we highly recommend to incubate with DCFH probe before exposing the cells to NMs.

We also recommend the use of a different positive control, as SIN-1 proved to be an unsuitable chemical positive control for this assay. SIN-1 is indeed a very potent inducer of ROS as seen by its direct activation of CM-H₂DCFDA-AE in our results, in previous research (He et al., 2018), and when used in an acellular protocol (Boyles et al., 2022), but RAW264.7 cells seem not to be susceptible or sensitive enough to this stress, showing only a slight increase in intracellular ROS at a dose 20-fold higher than the dose suggested in the ISO standard. We recommend PS-NH₂ as a positive control in this assay.

Another recommendation for improving the ISO protocol is to include an appropriate gating and analysis strategy. Especially since the assay is specifically made for NMs, which may be counted as events during flow cytometry when present in agglomerates or aggregates. The application of a singlets gate to exclude any doublets (two cells clumped together, leading to a doubling of the fluorescence signal) is highly recommended, as well as the inclusion of a live-death staining. Dead apoptotic cells are known to auto-fluoresce and should therefore be gated out. Additionally, Cytochrome C, which is released from the mitochondria during apoptosis, is able to oxidize DCFH, which could lead to an overestimation of the ROS production (Burkitt and Wardman, 2001).

Various nuances important to consider when performing the cellular DCFH assay have been shown and thoroughly discussed in this paper. The discovered issues together make the DCFH assay prone to misinterpretation, and results should be considered with caution to avoid

incorrect conclusions (Dikalov and Harrison, 2014; Kalyanaraman et al., 2012; Zielonka and Kalyanaraman, 2008). In terms of practical considerations for NMs, it is important to note that bovine serum albumin (BSA, occasionally used for NM dispersions) has been shown to directly bind DCF and thereby quenches the fluorescent signal (Subramaniam et al., 2002). Additionally, the ISO standard states that the DCFH probe is deactivated by serum, and serum should therefore be avoided during incubations (ISO, 2016). And finally for NMs specifically, additional controls should always be included (Aranda et al., 2013). Further recommendations on testing ROS and OS are given by Murphy et al. (Murphy et al., 2022).

4.3. Application of the DCFH assay for hazard screening purposes

Since the DCFH probe molecule does not detect any specific type of ROS, and is therefore able to give a more general indication of intracellular ROS, the DCFH assay is a good candidate for a hazard screening strategy in combination with other assays. This is of course when taking into consideration the currently presented optimizations of the assay, and when using an appropriate experimental setup and read-out method.

4.3.1. Cellular testing vs acellular testing

For the purpose of SSbD hazard testing, early hazard screening, and grouping and read-across, measuring acellular oxidative potential (OP) might be preferred over measuring cellular ROS, as it is easier and more cost-effective (Ruijter et al., 2023). An ISO standard is also available for acellular electronic spin resonance (ESR) analysis for NMs (ISO 18827:2017). An advantage of measuring in a cellular environment is that it takes into account the cellular antioxidant defence mechanisms, as well as mechanisms other than OP leading to ROS and oxidative stress (Hellack et al., 2017). Generally speaking, cellular ROS assays are better capable of predicting *in vivo* inflammatory effects as compared to acellular OP assays (Bahl et al., 2020; Hellack et al., 2017; Riebeling et al., 2016), but the prediction accuracy of the cellular DCFH assay has thus far not been studied.

In the case of the PS-NH $_2$ used in this study, it is known that it causes oxidative stress and cytotoxicity in RAW264.7 macrophages through lysosomal permeabilization upon particle uptake (Xia et al., 2008). This effect would not have been detected using acellular assays, as PS-NH $_2$ does not induce a reaction in an acellular environment (Xia et al., 2006). Additionally, here we show that the highly reactive SIN-1, which is a commonly used positive control in the acellular DCFH assay, only induced a slight increase in intracellular fluorescence at the highest exposure dose. This suggests that RAW264.7 macrophages are likely capable of coping with the specific type of stress induced by SIN-1. This would not have been noticed when measuring ROS induction in an acellular assay only.

RAW264.7 cells are used in ISO/TS 19006:2016 (ISO, 2016), and are therefore used in this paper as well. However, in literature the DCFH assay is performed on a wide range of cell types. ISO/TS 19006:2016 lists the following cell lines as appropriate alternatives: BEAS-2B, RLE-6TN, HEPA-1, HMEC, and A10 cell lines (ISO, 2016). The effectiveness of the assay might depend on the chosen cell type.

4.3.2. Simplicity

For an assay to be suitable for SSbD hazard testing, it should be simple due to the fact that its intended use is during the early stages of product development. A balance will always have to be established between the simplicity and sensitivity of chosen assays. In the case of the DCFH assay, use of a flow cytometer will enhance sensitivity, but will also detract from its simplicity, and makes it unsuitable for high throughput screening purposes. Additionally, most labs have access to a plate-reader but flow cytometers are expensive and not available for many labs. However, the findings in this paper question the suitability of the standard plate reader-based assay as a whole, and therefore

quantifying intracellular fluorescence using flow cytometry or using quantitative fluorescence microscopy should always be the preferred approach. The optimized flow cytometry-based DCFH protocol requires further evaluation in terms of sensitivity, specificity, and overall applicability domain in order to determine suitability for SSbD hazard screening purposes.

5. Conclusion

We have shown major pitfalls in the frequently used plate reader-based DCFH assay protocol to detect intracellular ROS and we show improvements of ISO/TS 19006:2016 to increase its reliability and sensitivity. We showed that both the fluorescent DCF as well as non-fluorescent metabolic products of the DCFH probe translocate from cells into the supernatant, and that CM-H₂DCFDA-AE is capable of reacting with commonly used positive controls in an acellular environment. The fluorescent signal observed in the plate reader-based protocol could be entirely attributed to a fluorescent supernatant, and not to the cells, making this assay very prone to misinterpretation. We conclude that using flow cytometry to measure fluorescence, incubating with DCFH probe before exposures to NMs, and using appropriate gating for data analysis, improve the performance of the DCFH assay. The optimized DCFH assay protocol presented in this paper could potentially be a useful addition to a hazard screening strategy in the context of SSbD after further assessment.

Funding

This research was funded by the SAbyNA Project, European Union's Horizon 2020 Research and Innovation Program under grant agreement No 862419, and by the Dutch Ministry of Infrastructure and Water Management.

CRediT authorship contribution statement

Nienke Ruijter: Conceptualization, Methodology, Investigation, Writing – original draft, Visualization. Margriet van der Zee: Conceptualization, Methodology, Supervision, Writing – review & editing. Alberto Katsumiti: Investigation, Writing – review & editing. Matthew Boyles: Investigation, Writing – review & editing. Flemming R. Cassee: Supervision, Writing – review & editing. Hedwig Braakhuis: Supervision, Writing – review & editing, Funding acquisition.

Declaration of competing interest

The authors certify that they have no affiliations with or involvement in any organization or entity with any financial interest (such as honoraria; educational grants; participation in speakers' bureaus; membership, employment, consultancies, stock ownership, or other equity interest; and expert testimony or patent-licensing arrangements) in the subject matter or materials discussed in this report apart from being employed by the National Institute for Public Health and the Environment - RIVM.

Data availability

Data will be made available on request.

Acknowledgements

The authors would like to thank Daan Lensen of the Centre for Health Protection at the RIVM for performing the LC-MS experiments and helping with the interpretation of the results; Arnout Hartendorp of the Centre for Health Protection at the RIVM for helping with the interpretation of the LC-MS results; Ronald Jacobi of the Centre for Immunology, Infectious Diseases and Vaccines at the RIVM for his help with setting up the flow cytometry analysis, and with troubleshooting even

outside of working hours; and Harm Heusinkveld of the Centre for Health Protection at the RIVM for his helpful insights and suggestions.

Appendix A. Supplementary data

Supplementary data to this article can be found online at https://doi.org/10.1016/j.impact.2024.100521.

References

- Abdal Dayem, A., Hossain, M.K., Lee, S.B., Kim, K., Saha, S.K., Yang, G.M., Choi, H.Y., Cho, S.G., 2017. The role of reactive oxygen species (ROS) in the biological activities of metallic nanoparticles. Int. J. Mol. Sci. 18 (1) https://doi.org/10.3390/ iims18010120
- Ag Seleci, D., Tsiliki, G., Werle, K., Elam, D.A., Okpowe, O., Seidel, K., Bi, X., Westerhoff, P., Innes, E., Boyles, M., Miller, M., Giusti, A., Murphy, F., Haase, A., Stone, V., Wohlleben, W., 2022. Determining nanoform similarity via assessment of surface reactivity by abiotic and in vitro assays. NanoImpact 26, 100390. https://doi.org/10.1016/j.impact.2022.100390.
- Aranda, A., Sequedo, L., Tolosa, L., Quintas, G., Burello, E., Castell, J.V., Gombau, L., 2013. Dichloro-dihydro-fluorescein diacetate (DCFH-DA) assay: a quantitative method for oxidative stress assessment of nanoparticle-treated cells. Toxicol. In Vitro 27 (2), 954–963. https://doi.org/10.1016/j.tiv.2013.01.016.
- Arts, J.H., Hadi, M., Irfan, M.A., Keene, A.M., Kreiling, R., Lyon, D., Maier, M., Michel, K., Petry, T., Sauer, U.G., Warheit, D., Wiench, K., Wohlleben, W., Landsiedel, R., 2015. A decision-making framework for the grouping and testing of nanomaterials (DF4nanoGrouping). Regul. Toxicol. Pharmacol. 71 (2 Suppl), S1–27. https://doi.org/10.1016/j.yrtph.2015.03.007.
- Ayres, J.G., Borm, P., Cassee, F.R., Castranova, V., Donaldson, K., Ghio, A., Harrison, R. M., Hider, R., Kelly, F., Kooter, I.M., Marano, F., Maynard, R.L., Mudway, I., Nel, A., Sioutas, C., Smith, S., Baeza-Squiban, A., Cho, A., Duggan, S., Froines, J., 2008. Evaluating the toxicity of airborne particulate matter and nanoparticles by measuring oxidative stress potential—a workshop report and consensus statement. Inhal. Toxicol. 20 (1), 75–99. https://doi.org/10.1080/08958370701665517.
- Bahl, A., Hellack, B., Wiemann, M., Giusti, A., Werle, K., Haase, A., Wohlleben, W., 2020. Nanomaterial categorization by surface reactivity: a case study comparing 35 materials with four different test methods. NanoImpact 19. https://doi.org/10.1016/j.impact.2020.100234.
- Bass, D.A., Parce, J.W., Dechatelet, L.R., Szejda, P., Seeds, M.C., Thomas, M., 1983. Flow cytometric studies of oxidative product formation by neutrophils: a graded response to membrane stimulation. J. Immunol. 130 (4), 1910–1917.
- Botte, E., Vagaggini, P., Zanoni, I., Gardini, D., Costa, A.L., Ahluwalia, A.D., 2021. An integrated pipeline and multi-model graphical user interface for accurate nanodosimetry. bioRxiv 2021–08. https://doi.org/10.1101/2021.08.31.458389.
- Boyles, M., Murphy, F., Mueller, W., Wohlleben, W., Jacobsen, N.R., Braakhuis, H., Giusti, A., Stone, V., 2022. Development of a standard operating procedure for the DCFH2-DA acellular assessment of reactive oxygen species produced by nanomaterials. Toxicol. Mech. Methods 32 (6), 439–452. https://doi.org/10.1080/ 15376516.2022.2029656.
- Braakhuis, H.M., Giannakou, C., Peijnenburg, W.J., Vermeulen, J., van Loveren, H., Park, M.V., 2016. Simple in vitro models can predict pulmonary toxicity of silver nanoparticles. Nanotoxicology 10 (6), 770–779. https://doi.org/10.3109/17435390.2015.1127443.
- Braakhuis, H.M., Gosens, I., Heringa, M.B., Oomen, A.G., Vandebriel, R.J., Groenewold, M., Cassee, F.R., 2020. Mechanism of action of TiO2: recommendations to reduce uncertainties related to carcinogenic potential. Annu. Rev. Pharmacol. Toxicol. https://doi.org/10.1146/annurev-pharmtox-101419-100049.
- Braakhuis, H.M., Murphy, F., Ma-Hock, L., Dekkers, S., Keller, J., Oomen, A.G., Stone, V., 2021. An integrated approach to testing and assessment to support grouping and read-across of nanomaterials after inhalation exposure. Appl In Vitro Toxicol 7 (3), 112–128. https://doi.org/10.1089/ajvt_2021.0009.
- Burkitt, M.J., Wardman, P., 2001. Cytochrome C is a potent catalyst of dichlorofluorescin oxidation: implications for the role of reactive oxygen species in apoptosis. Biochem. Biophys. Res. Commun. 282 (1), 329–333. https://doi.org/10.1006/bbrc.2001.4578.
- Caldeira, C., Farcal, R., Garmendia, A.I., Mancini, L., Tosches, D., Amelio, A., Rasmussen, K., Rauscher, H., Riego, S.J., Sala, S., 2022. Safe and Sustainable by Design Chemicals and Materials-Framework for the Definition of Criteria and Evaluation Procedure for Chemicals and Materials (9276532641).
- Croissant, J.G., Butler, K.S., Zink, J.I., Brinker, C.J., 2020. Synthetic amorphous silica nanoparticles: toxicity, biomedical and environmental implications. Nat. Rev. Mater. 5 (12), 886–909.
- Dekkers, S., Oomen, A.G., Bleeker, E.A., Vandebriel, R.J., Micheletti, C., Cabellos, J., Janer, G., Fuentes, N., Vazquez-Campos, S., Borges, T., Silva, M.J., Prina-Mello, A., Movia, D., Nesslany, F., Ribeiro, A.R., Leite, P.E., Groenewold, M., Cassee, F.R., Sips, A.J., Wijnhoven, S.W., 2016. Towards a nanospecific approach for risk assessment. Regul. Toxicol. Pharmacol. 80, 46–59. https://doi.org/10.1016/j. yrtph.2016.05.037.
- Dekkers, S., Wijnhoven, S.W.P., Braakhuis, H.M., Soeteman-Hernandez, L.G., Sips, A.J.A. M., Tavernaro, I., Kraegeloh, A., Noorlander, C.W., 2020. Safe-by-design part I: proposal for nanospecific human health safety aspects needed along the innovation process. NanoImpact 18. https://doi.org/10.1016/j.impact.2020.100227.

- DeLoid, G.M., Cohen, J.M., Pyrgiotakis, G., Demokritou, P., 2017. Preparation, characterization, and in vitro dosimetry of dispersed, engineered nanomaterials. Nat. Protoc. 12 (2), 355–371. https://doi.org/10.1038/nprot.2016.172.
- Di Cristo, L., Oomen, A.G., Dekkers, S., Moore, C., Rocchia, W., Murphy, F., Johnston, H. J., Janer, G., Haase, A., Stone, V., Sabella, S., 2021. Grouping hypotheses and an integrated approach to testing and assessment of nanomaterials following oral ingestion. Nanomaterials 11 (10), 2623. https://www.mdpi.com/2079-4991/11/10/2623
- Dikalov, S.I., Harrison, D.G., 2014. Methods for detection of mitochondrial and cellular reactive oxygen species. Antioxid. Redox Signal. 20 (2), 372–382. https://doi.org/ 10.1089/ars.2012.4886.
- Folkes, L.K., Patel, K.B., Wardman, P., Wrona, M., 2009. Kinetics of reaction of nitrogen dioxide with dihydrorhodamine and the reaction of the dihydrorhodamine radical with oxygen: implications for quantifying peroxynitrite formation in cells. Arch. Biochem. Biophys. 484 (2), 122–126. https://doi.org/10.1016/j.abb.2008.10.014.
- Fu, P.P., Xia, Q., Hwang, H.M., Ray, P.C., Yu, H., 2014. Mechanisms of nanotoxicity: generation of reactive oxygen species. J. Food Drug Anal. 22 (1), 64–75. https://doi. org/10.1016/j.jfda.2014.01.005.
- Guadagnini, R., Halamoda Kenzaoui, B., Walker, L., Pojana, G., Magdolenova, Z., Bilanicova, D., Saunders, M., Juillerat-Jeanneret, L., Marcomini, A., Huk, A., Dusinska, M., Fjellsbo, L.M., Marano, F., Boland, S., 2015. Toxicity screenings of nanomaterials: challenges due to interference with assay processes and components of classic in vitro tests. Nanotoxicology 9 (Suppl. 1), 13–24. https://doi.org/ 10.3109/17435390.2013.829590.
- Gulumian, M., Cassee, F.R., 2021. Safe by design (SbD) and nanotechnology: a much-discussed topic with a prudence? Part. Fibre Toxicol. 18 (1), 32. https://doi.org/10.1186/s12989-021-00423-0.
- Halappanavar, S., Nymark, P., Krug, H.F., Clift, M.J.D., Rothen-Rutishauser, B., Vogel, U., 2021. Non-animal strategies for toxicity assessment of nanoscale materials: role of adverse outcome pathways in the selection of endpoints. Small 17 (15), e2007628. https://doi.org/10.1002/smll.202007628.
- He, Y., Zhang, Y., Zhang, D., Zhang, M., Wang, M., Jiang, Z., Otero, M., Chen, J., 2018. 3-morpholinosydnonimine (SIN-1)-induced oxidative stress leads to necrosis in hypertrophic chondrocytes in vitro. Biomed. Pharmacother. 106, 1696–1704. https://doi.org/10.1016/j.biopha.2018.07.128.
- Hellack, B., Nickel, C., Albrecht, C., Kuhlbusch, T.A.J., Boland, S., Baeza-Squiban, A., Wohlleben, W., Schins, R.P.F., 2017. Analytical methods to assess the oxidative potential of nanoparticles: a review. Environ. Sci. Nano 4 (10), 1920–1934. https://doi.org/10.1039/c7en00346c.
- Heusinkveld, H.J., Westerink, R.H.S., 2011. Caveats and limitations of plate reader-based high-throughput kinetic measurements of intracellular calcium levels. Toxicol. Appl. Pharmacol. 255 (1), 1–8. https://doi.org/10.1016/j.taap.2011.05.020.
- Inshakova, E., Inshakov, O., 2017. World Market for Nanomaterials: Structure and Trends (MATEC web of conferences).
- ISO, 2016. Nanotechnologies 5-(and 6)-Chloromethyl-2,7 Dichloro-dihydrofluorescein diacetate (CMH2DCF-DA) assay for evaluating nanoparticle-induced intracellular reactive oxygen species (ROS) production in RAW 264.7 macrophage cell line (ISO/ TS 19006-2016 IDT)
- Jensen, K., 2018. The NANOGENOTOX Standard Operational Procedure for Preparing Batch Dispersions for In Vitro and In Vivo Toxicological Studies. In: Version.
- Joris, F., Manshian, B.B., Peynshaert, K., De Smedt, S.C., Braeckmans, K., Soenen, S.J., 2013. Assessing nanoparticle toxicity in cell-based assays: influence of cell culture parameters and optimized models for bridging the in vitro-in vivo gap. Chem. Soc. Rev. 42 (21), 8339–8359. https://doi.org/10.1039/c3cs60145e.
- Kalyanaraman, B., Darley-Usmar, V., Davies, K.J., Dennery, P.A., Forman, H.J., Grisham, M.B., Mann, G.E., Moore, K., Roberts 2nd, L.J., Ischiropoulos, H., 2012. Measuring reactive oxygen and nitrogen species with fluorescent probes: challenges and limitations. Free Radic. Biol. Med. 52 (1), 1–6. https://doi.org/10.1016/j. freeradbiomed.2011.09.030.
- Koike, E., Kobayashi, T., 2006. Chemical and biological oxidative effects of carbon black nanoparticles. Chemosphere 65 (6), 946–951. https://doi.org/10.1016/j. chemosphere.2006.03.078.
- Kroll, A., Dierker, C., Rommel, C., Hahn, D., Wohlleben, W., Schulze-Isfort, C., Göbbert, C., Voetz, M., Hardinghaus, F., Schnekenburger, J., 2011. Cytotoxicity screening of 23 engineered nanomaterials using a test matrix of ten cell lines and three different assays. Part. Fibre Toxicol. 8, 9. https://doi.org/10.1186/1743-8977-8-9.
- Kroll, A., Pillukat, M.H., Hahn, D., Schnekenburger, J., 2012. Interference of engineered nanoparticles with in vitro toxicity assays. Arch. Toxicol. 86 (7), 1123–1136. https://doi.org/10.1007/s00204-012-0837-z.
- Murphy, M.P., Bayir, H., Belousov, V., Chang, C.J., Davies, K.J., Davies, M.J., Dick, T.P., Finkel, T., Forman, H.J., Janssen-Heininger, Y., 2022. Guidelines for measuring reactive oxygen species and oxidative damage in cells and in vivo. Nat. Metab. 4 (6), 651–662.
- OECD, 2020. Moving Towards a Safe(r) Innovation Approach (SIA) for More Sustainable Nanomaterials and Nano-enabled Products. Series on the Safety of Manufactured Nanomaterials, Issue. https://www.oecd.org/officialdocuments/publicdisplaydocumentpdf/?cote=env/jm/mono(2020)36/REV1&doclanguage=en.
- Ohashi, T., Mizutani, A., Murakami, A., Kojo, S., Ishii, T., Taketani, S., 2002. Rapid oxidation of dichlorodihydrofluorescin with heme and hemoproteins: formation of the fluorescein is independent of the generation of reactive oxygen species. FEBS Lett. 511 (1), 21–27. https://doi.org/10.1016/S0014-5793(01)03262-8.
- Pal, A.K., Hsieh, S.-F., Khatri, M., Isaacs, J.A., Demokritou, P., Gaines, P., Schmidt, D.F., Rogers, E.J., Bello, D., 2014. Screening for oxidative damage by engineered nanomaterials: a comparative evaluation of FRAS and DCFH. J. Nanopart. Res. 16 (2), 2167. https://doi.org/10.1007/s11051-013-2167-3.

- Reddy, A.R., Rao, M.V., Krishna, D.R., Himabindu, V., Reddy, Y.N., 2011. Evaluation of oxidative stress and anti-oxidant status in rat serum following exposure of carbon nanotubes. Regul. Toxicol. Pharmacol. 59 (2), 251–257. https://doi.org/10.1016/j. yrtph.2010.10.007.
- Reiniers, M.J., de Haan, L.R., Reeskamp, L.F., Broekgaarden, M., van Golen, R.F., Heger, M., 2021. Analysis and optimization of conditions for the use of 2', 7'dichlorofluorescein diacetate in cultured hepatocytes. Antioxidants 10 (5), 674.
- Ribeiro, A.R., Leite, P.E., Falagan-Lotsch, P., Benetti, F., Micheletti, C., Budtz, H.C., Jacobsen, N.R., Lisboa-Filho, P.N., Rocha, L.A., Kühnel, D., Hristozov, D., Granjeiro, J.M., 2017. Challenges on the toxicological predictions of engineered nanoparticles. NanoImpact 8, 59–72. https://doi.org/10.1016/j.impact 2017 07 006
- Richter, K., Kietzmann, T., 2016. Reactive oxygen species and fibrosis: further evidence of a significant liaison. Cell Tissue Res. 365, 591–605.
- Riebeling, C., Wiemann, M., Schnekenburger, J., Kuhlbusch, T.A.J., Wohlleben, W., Luch, A., Haase, A., 2016. A redox proteomics approach to investigate the mode of action of nanomaterials. Toxicol. Appl. Pharmacol. 299, 24–29. https://doi.org/ 10.1016/j.taap.2016.01.019.
- Ruijter, N., Soeteman-Hernández, L.G., Carrière, M., Boyles, M., McLean, P., Catalán, J., Katsumiti, A., Cabellos, J., Delpivo, C., Sánchez Jiménez, A., 2023. The state of the art and challenges of in vitro methods for human Hazard assessment of nanomaterials in the context of safe-by-design. Nanomaterials 13 (3), 472.
- Saber, A.T., Jensen, K.A., Jacobsen, N.R., Birkedal, R., Mikkelsen, L., Moller, P., Loft, S., Wallin, H., Vogel, U., 2012. Inflammatory and genotoxic effects of nanoparticles designed for inclusion in paints and lacquers. Nanotoxicology 6 (5), 453–471. https://doi.org/10.3109/17435390.2011.587900.
- Saikolappan, S., Kumar, B., Shishodia, G., Koul, S., Koul, H.K., 2019. Reactive oxygen species and cancer: a complex interaction. Cancer Lett. 452, 132–143. https://doi. org/10.1016/j.canlet.2019.03.020.
- Shen, Y., Wu, L., Qin, D., Xia, Y., Zhou, Z., Zhang, X., Wu, X., 2018. Carbon black suppresses the osteogenesis of mesenchymal stem cells: the role of mitochondria. Particle and fibre toxicology 15, 1–17.
- Soeteman-Hernandez, L.G., Apostolova, M.D., Bekker, C., Dekkers, S., Grafström, R.C., Groenewold, M., Handzhiyski, Y., Herbeck-Engel, P., Hoehener, K., Karagkiozaki, V., Kelly, S., Kraegeloh, A., Logothetidis, S., Micheletti, C., Nymark, P., Oomen, A., Oosterwijk, T., Rodríguez-Llopis, I., Sabella, S., Noorlander, C.W., 2019. Safe innovation approach: towards an agile system for dealing with innovations. Materials Today Communications 20. https://doi.org/10.1016/j.mtcomm.2019.100548.
- Stone, V., Gottardo, S., Bleeker, E.A.J., Braakhuis, H., Dekkers, S., Fernandes, T., Haase, A., Hunt, N., Hristozov, D., Jantunen, P., Jeliazkova, N., Johnston, H., Lamon, L., Murphy, F., Rasmussen, K., Rauscher, H., Jiménez, A.S., Svendsen, C., Spurgeon, D., Oomen, A.G., 2020. A framework for grouping and read-across of nanomaterials- supporting innovation and risk assessment. Nano Today 35. https://doi.org/10.1016/j.nantod.2020.100941.
- Subramaniam, R., Fan, X.-J., Scivittaro, V., Yang, J., Ha, C.-E., Petersen, C.E., Surewicz, W.K., Bhagavan, N.V., Weiss, M.F., Monnier, V.M., 2002. Cellular oxidant stress and advanced glycation endproducts of albumin: caveats of the

- Dichlorofluorescein assay*. Arch. Biochem. Biophys. 400 (1), 15–25. https://doi.org/10.1006/abbi.2002.2776.
- Suzuki, H., Toyooka, T., Ibuki, Y., 2007. Simple and easy method to evaluate uptake potential of nanoparticles in mammalian cells using a flow cytometric light scatter analysis. Environ. Sci. Technol. 41 (8), 3018–3024. https://doi.org/10.1021/ es0625632.
- van Berlo, D., Wessels, A., Boots, A.W., Wilhelmi, V., Scherbart, A.M., Gerloff, K., van Schooten, F.J., Albrecht, C., Schins, R.P., 2010. Neutrophil-derived ROS contribute to oxidative DNA damage induction by quartz particles. Free Radic. Biol. Med. 49 (11), 1685–1693. https://doi.org/10.1016/j.freeradbiomed.2010.08.031.
- Vranic, S., Gosens, I., Jacobsen, N.R., Jensen, K.A., Bokkers, B., Kermanizadeh, A., Stone, V., Baeza-Squiban, A., Cassee, F.R., Tran, L., Boland, S., 2017. Impact of serum as a dispersion agent for in vitro and in vivo toxicological assessments of TiO2 nanoparticles. Arch. Toxicol. 91 (1), 353–363. https://doi.org/10.1007/s00204-016-1673-3
- Wan, C.P., Myung, E., Lau, B.H., 1993. An automated micro-fluorometric assay for monitoring oxidative burst activity of phagocytes. J. Immunol. Methods 159 (1–2), 131–138. https://doi.org/10.1016/0022-1759(93)90150-6.
- Wang, H., Joseph, J.A., 1999. Quantifying cellular oxidative stress by dichlorofluorescein assay using microplate reader. Free Radic. Biol. Med. 27 (5–6), 612–616. https://doi. org/10.1016/s0891-5849(99)00107-0.
- Wang, Y., Zhang, Y., Guo, Y., Lu, J., Veeraraghavan, V.P., Mohan, S.K., Wang, C., Yu, X., 2019. Synthesis of zinc oxide nanoparticles from Marsdenia tenacissima inhibits the cell proliferation and induces apoptosis in laryngeal cancer cells (Hep-2). J. Photochem. Photobiol. B Biol. 201, 111624.
- Wardman, P., 2007. Fluorescent and luminescent probes for measurement of oxidative and nitrosative species in cells and tissues: Progress, pitfalls, and prospects. Free Radic. Biol. Med. 43 (7), 995–1022. https://doi.org/10.1016/j. freeradbiomed.2007.06.026.
- Xia, T., Kovochich, M., Brant, J., Hotze, M., Sempf, J., Oberley, T., Sioutas, C., Yeh, J.I., Wiesner, M.R., Nel, A.E., 2006. Comparison of the abilities of ambient and manufactured nanoparticles to induce cellular toxicity according to an oxidative stress paradigm. Nano Lett. 6 (8), 1794–1807. https://doi.org/10.1021/nl061025k.
- Xia, T., Kovochich, M., Liong, M., Zink, J.I., Nel, A.E., 2008. Cationic polystyrene nanosphere toxicity depends on cell-specific endocytic and mitochondrial injury pathways. ACS Nano 2 (1), 85–96. https://doi.org/10.1021/nn700256c.
- Zhang, X., Gao, F., 2015. Imaging mitochondrial reactive oxygen species with fluorescent probes: current applications and challenges. Free Radic. Res. 49 (4), 374–382. https://doi.org/10.3109/10715762.2015.1014813.
- Zielinska, A., Costa, B., Ferreira, M.V., Migueis, D., Louros, J.M.S., Durazzo, A., Lucarini, M., Eder, P., Chaud, M.V., Morsink, M., Willemen, N., Severino, P., Santini, A., Souto, E.B., 2020. Nanotoxicology and nanosafety: safety-by-design and testing at a glance. Int. J. Environ. Res. Public Health 17 (13). https://doi.org/10.3390/ijerph17134657.
- Zielonka, J., Kalyanaraman, B., 2008. "ROS-generating mitochondrial DNA mutations can regulate tumor cell metastasis"—a critical commentary. Free Radical Biology and Medicine 45 (9), 1217–1219.